nature neuroscience

Microcircuitry coordination of cortical motor information in self-initiation of voluntary movements

Yoshikazu Isomura[1], Rie Harukuni[1], Takashi Takekawa[1], Hidenori Aizawa[2] & Tomoki Fukai[1,3,4]

Motor cortex neurons are activated at different times during self-initiated voluntary movement. However, the manner in which excitatory and inhibitory neurons in distinct cortical layers help to organize voluntary movement is poorly understood. We carried out juxtacellular and multiunit recordings from actively behaving rats and found temporally and functionally distinct activations of excitatory pyramidal cells and inhibitory fast-spiking interneurons. Across cortical layers, pyramidal cells were activated diversely for sequential motor phases (for example, preparation, initiation and execution). In contrast, fast-spiking interneurons, including parvalbumin-positive basket cells, were recruited predominantly for motor execution, with pyramidal cells producing a command-like activity. Thus, fast-spiking interneurons may underlie command shaping by balanced inhibition or recurrent inhibition, rather than command gating by temporally alternating excitation and inhibition. Furthermore, initiation-associated pyramidal cells excited similar and different functional classes of neurons through putative monosynaptic connections. This suggests that these cells may temporally integrate information to initiate and coordinate voluntary movement.

The primary motor cortex changes its neural activity, as seen via electroencephalography, much earlier than the onset of spontaneous voluntary movement[1,2]. In primates[3,4] and rodents[5–7], motor cortex neurons are activated or inactivated both long before and during movement expression. The temporally differential activation of these neurons might correspond to sequential phases of single voluntary movement, such as motor preparation, initiation, execution and termination/switch. Antidromic identification techniques can characterize the discharge activity of corticofugal neurons long-projecting to the spinal cord[3,4,8–10], striatum[8,9] and red nucleus[10] during voluntary movements. However, very few attempts have been made to elucidate the intracortical mechanism underlying motor-command generation for voluntary movement because direct morphological identification of recorded neurons has been technically difficult in actively behaving animals.

In the forelimb area of the rat motor cortex[11–13], layer 2/3 pyramidal cells principally project to other cortical areas, layer 5 pyramidal cells project to subcortical structures such as the spinal cord and the striatum, and layer 6 pyramidal cells project to thalamic nuclei. These excitatory pyramidal cells, along with the star-like pyramidal cells in layer 4 of the forelimb area, also innervate local cortico-spinal pyramidal cells in layer 5 via axon collaterals[14,15]. An *in vitro* analysis of excitatory laminar connectivity predicted that motor information primarily flows from layer 2/3 to layer 5 circuit of the motor cortex[16]. On the other hand, a major population of nonpyramidal, inhibitory GABAergic interneurons consists of fast-spiking interneurons (mostly basket cells and chandelier cells), which fire narrow action potentials at a fast rate and usually express parvalbumin[17]. These interneurons might gate spike outputs from the pyramidal cells with powerful inhibitory synapses on somata or axons[18]. A single-unit study reported that putative layer 5 pyramidal cells and putative fast-spiking interneurons of the rabbit motor cortex discharge in an antiphasic manner during locomotion cycles[19]. Locomotion, however, consists of continuous and complex limb movements and is driven by subcortical pattern generator(s) under cortical controls. Therefore, the manner in which excitatory pyramidal cells and inhibitory interneurons in the different layers of the motor cortex process sequential motor information along the temporal flow of single voluntary movement remains a mystery.

To address these issues, we carried out juxtacellular and multiunit recordings from the motor cortex in head-restrained rats that were trained to spontaneously repeat forelimb movements. The juxtacellular recording technique provides accurate spike events and morphological features for a cortical[20–22] or subcortical neuron[23,24]. The multiunit recording technique is useful for obtaining spike events of many neurons simultaneously[25–27] and for exploring their synaptic connectivity[28–31] in a blind and unbiased manner. Our experimental approach uncovered the functional diversity of pyramidal cells and uniformity of fast-spiking interneurons across all cortical layers in the expression of voluntary movement. Furthermore, we found a pattern of excitatory synaptic interactions among neighboring neurons that have different roles in self-initiated movement.

RESULTS

Functional activations in motor cortex neurons

To obtain a sufficient number of task-trained rats for juxtacellular visualization, we developed a multi-rat task-training system to simultaneously train up to six adult rats on an operant

[1]Neural Circuit Theory and [2]Developmental Gene Regulation, RIKEN Brain Science Institute, Wako, Saitama, Japan. [3]Complexity Science and Engineering, University of Tokyo, Kashiwa, Chiba, Japan. [4]Brain Research Center, Tamagawa University, Machida, Tokyo, Japan. Correspondence should be addressed to Y.I. (isomura@brain.riken.jp).

Received 27 March; accepted 25 September; published online 8 November 2009; doi:10.1038/nn.2431

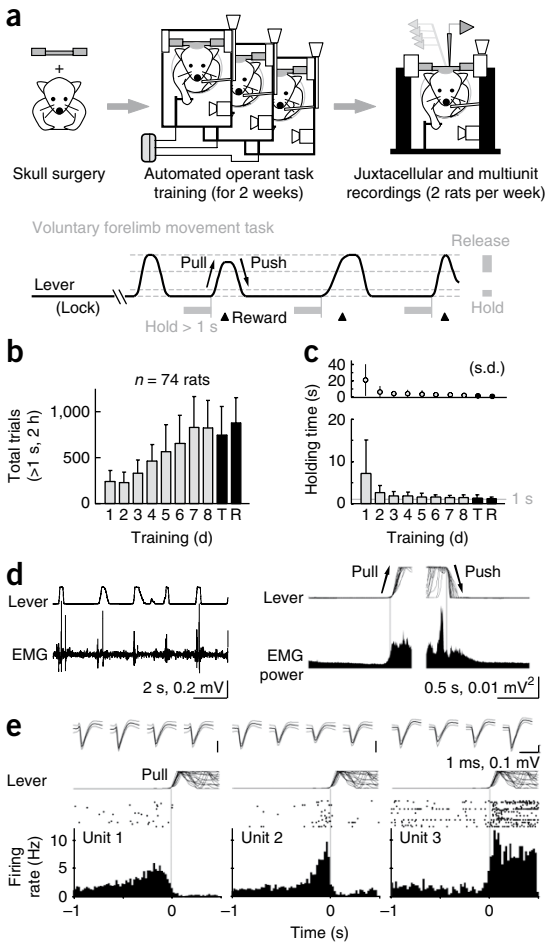

Figure 1 Efficient operant learning of the voluntary forelimb-movement task. (**a**) Schematic diagram of juxtacellular and multiunit recordings from the forelimb area of head-restraint rats that were trained to perform a voluntary (self paced) forelimb-movement task using our multi-rat task-training system. (**b**) Increase in the total number of successful trials during the 2-week training period ($n = 74$ rats, mean and s.d.). (**c**) The convergence of lever-holding time toward 1 s (lower) with less s.d. (upper) over time. R, recording day; T, room transfer day. (**d**) Left, lever trajectory and electromyogram (EMG) activity in the right forelimb during task performance. Right, averaged EMG power aligned to the onset of pull or push movements (vertical line). (**e**) Three representative neurons with distinct firing activity in relation to pull movement. These neurons were recorded simultaneously through the same multiunit electrode. Top, spike waveform for each channel. Middle, lever trajectories. Bottom, task-related firing activity aligned at the onset (0 s) of pull movement (20-ms bins).

voluntary forelimb-movement task (**Fig. 1a**). After primary surgery (**Supplementary Fig. 1**), the trainee rats did not struggle under a head-restraint condition, instead grasping a lever with their right forelimb in a properly relaxed posture and quickly learning the causal relation between lever movement and reward water in the operant trials (**Supplementary Fig. 2** and **Supplementary Video 1**). All 74 rats learned to perform the operant motor task in 2 weeks (8 d of training, 825 ± 302 trials, holding time of 1.42 ± 0.64 s for 2 h on the eighth day; **Fig. 1b**,**c**, **Supplementary Fig. 3** and **Supplementary Video 2**). The rats were then transferred to a recording room where they performed the same motor task during juxtacellular and multiunit recordings from the left forelimb area (879 ± 282 trials, holding time of 1.18 ± 0.34 s; **Supplementary Fig. 4**). In each trial, the forelimb muscles (for example, biceps brachii) became active just before the onset of pull movement (**Fig. 1d** and **Supplementary Fig. 4**). Consistent with previous studies[6,7], our multiunit recordings revealed several distinct patterns of neuronal firing at an electrode site in relation to the forelimb-movement task (**Fig. 1e**). It is unlikely that the different firing patterns merely represented different muscular movements, as they were recorded simultaneously in the same somatotopic position of motor cortex[11–13]; in addition, forelimb movements occurred much later and more rapidly than the slowly increasing activity of these neurons (**Fig. 1d**,**e**).

We further investigated the variety of motor task–related neuronal firing by juxtacellular recording (**Supplementary Fig. 5**). We classified firing into five temporally and functionally distinct patterns of task-related activity in pyramidal cells identified in the forelimb area: hold-related, pre-movement, movement, movement-off and post-movement activity. Hold-related activity, which might be involved in motor preparation or stillness, showed a gradually increasing or decreasing activation during the immovable (that is, lever holding) state (**Fig. 2a**). Pre-movement activity, which might be involved in motor initiation, was phasic and preceded the onset of pull or push movement; the activity was then rapidly decreased during movement expression (**Fig. 2b**). Two well-visualized, deep-layer pyramidal cells showing pre-movement activity extended their axons into subcortical structures (**Fig. 2**; see also **Supplementary Fig. 6** and **Supplementary Video 3**), presumably to recruit cortico-subcortical loops, such as the basal ganglia, for motor initiation. Movement activity showed a typical command-like activation during the movement expression (**Fig. 2c**). This activity might contribute to motor execution and/or somatosensory feedback. Movement-off activity showed a sudden depression of tonic and constant firing during the movement expression (**Fig. 2d**). Pyramidal cells displaying movement-off activity included a spiny, star-like pyramidal cell in layer 4 of the forelimb area[14,15] (**Fig. 2d**,**g**); this suggested that the activity might be related to input gating or modulation. Post-movement activity showed a brief activation at the end of the movement (**Fig. 2e**), possibly engaging in motor termination or switch. We found only one intrinsically bursting pyramidal cell in layer 3 (**Supplementary Fig. 6**) and the other pyramidal cells had the electrophysiological properties of regular-spiking neurons.

Whether the forelimb area of motor cortex (usually agranular) and that of somatosensory cortex (granular) are located very close to[13] or overlapping with[11,14,15] each other is not known. Our juxtacellular analysis suggests that they overlap, as identified pyramidal cells in the forelimb area containing layer 4 (that is, granular cortex) were activated in relation to motor preparation or initiation lacking sensory feedback (**Fig. 2a**,**b** and **Supplementary Figs. 4** and **6**).

We examined two representative interneurons with high-frequency movement activity in superficial and deep cortical layers, which we classified as parvalbumin-positive fast-spiking basket cells using morphological and electrophysiological methods (**Fig. 3**). Most of the fast-spiking interneurons obtained with juxtacellular and multiunit recordings were activated from the baseline level primarily during the expression of movement and showed lower selectivity to pull versus push movement than pyramidal cells (**Figs. 2c** and **3b**). We found no other subtypes of task-related interneurons juxtacellularly. This may be because these interneurons represent a smaller population and have lower firing activity or have less correlation with the task behavior.

Functional diversity in pyramidal cells and interneurons

We cleanly isolated[25,26] a total of 166 neurons from multiunit recordings in deep layers of the forelimb area. These neurons were

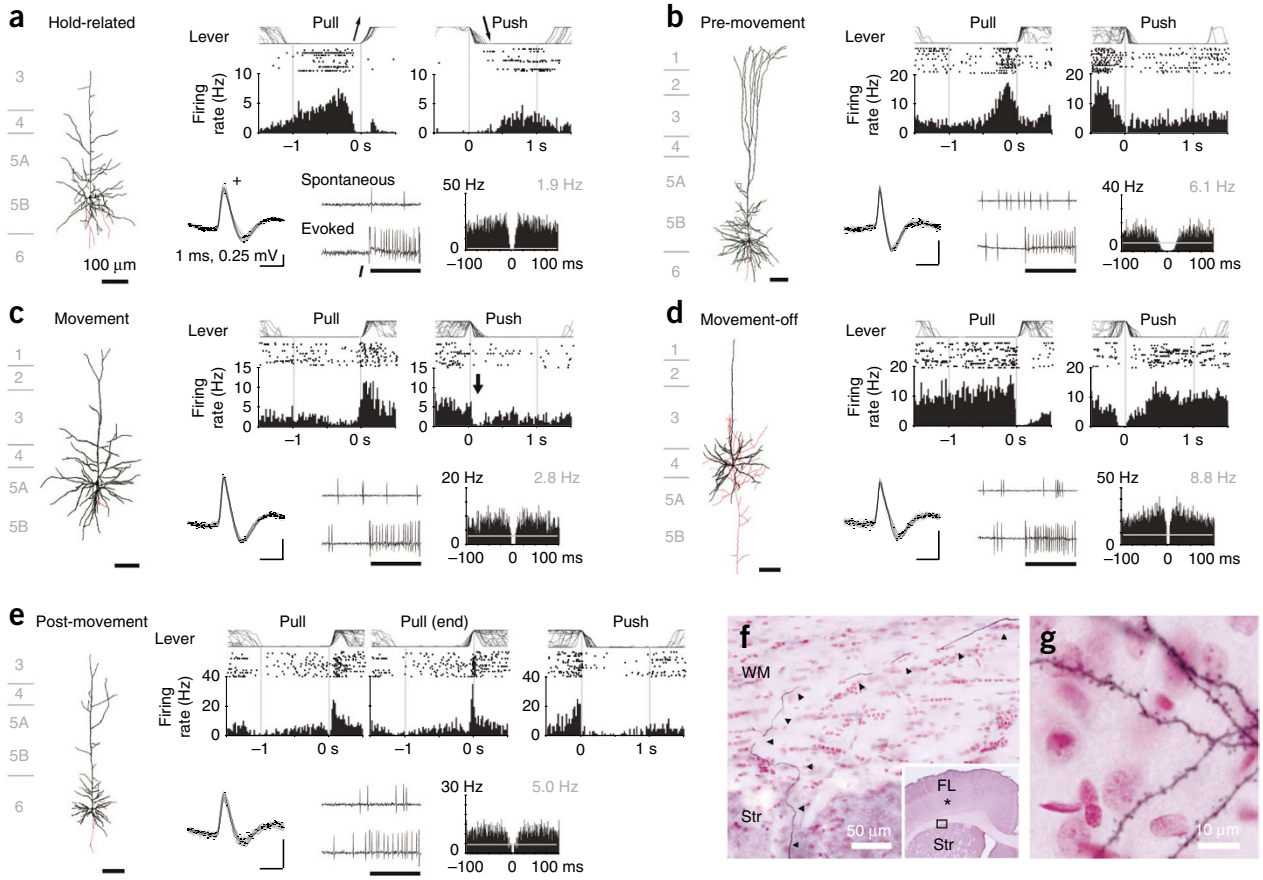

Figure 2 Diverse functional activation of identified pyramidal cells. (**a**) Layer 5B pyramidal cell showing a gradual increase in firing activity during lever holding and a decrease during pull and push movements (hold-related activity). Left, the morphology of the recorded neuron (black, soma and dendrites; red, axons). Top, task-related firing activity aligned at the onset of pull or push movement. Bottom, spike waveforms (left), spontaneous and evoked (*I*) spiking traces (middle), and auto-correlation histogram (right, 1-ms bins; gray, ongoing firing rate). +, positive. (**b**) Layer 5B pyramidal cell showing transiently increased activity just before the onset of pull movement (pre-movement activity). (**c**) Layer 5A pyramidal cell showing increased activity with pull movement (movement activity). Arrow indicates an activity reduction in the nonpreferred direction. (**d**) Layer 4, spiny, star-like pyramidal cell showing an abrupt decrease in tonic and constant firing during pull movement (movement-off activity). Note that layer 4 exists in the rat forelimb motor area[14,15]. (**e**) Layer 6 pyramidal cell showing a peak activity at the end of, rather than during, pull movement (post-movement activity). (**f**) Axons (triangles, reconstructed) running through the white matter (WM) and striatum (Str) from the neuron shown in **b**. Inset, location of the soma (asterisk). FL, forelimb area. (**g**) Spine-rich dendrites of the neuron shown in **d**.

divided into regular-spiking neurons (n = 150), which should mainly comprise excitatory pyramidal cells, and fast-spiking neurons (n = 16) on the basis of spike duration[30,31] (n = 22 rats; **Fig. 4a**). The regular-spiking population yielded a diverse range of task-related activity: 41 hold-related, 10 pre-movement, 51 movement, 14 movement-off, 3 post-movement and 31 non–task-related neurons (**Fig. 4a**). In contrast, the majority of fast-spiking neurons exhibited movement activity (13 movement, 1 pre-movement, 1 post-movement and 1 non–task-related neurons; χ^2 test, $P < 0.001$ between regular-spiking and fast-spiking for movement). The regular-spiking population, however, might include various non–fast-spiking interneurons[17,18], which cannot be distinguished from pyramidal cells with similar spike waveforms. Thus, non–fast-spiking interneurons may have contributed to the functional diversity of regular-spiking population.

Juxtacellular recordings provided stronger evidence for the difference between excitatory and inhibitory neuronal activity. Of 87 recorded neurons (n = 69 rats), 68 were injected with biocytin/Neurobiotin for morphological identification and 38 of these (56%) were visualized successfully. We identified these neurons as 27 task-related and 2 non–task-related pyramidal cells and 9 task-related (including 8 parvalbumin positive) fast-spiking interneurons. The remaining neurons were further classified as putative pyramidal cells (n = 41) and putative fast-spiking interneurons (n = 8, 1 non–task related) on the basis of the distribution of ongoing activity and spike width in identified neurons (**Fig. 4b**). Identified and putative pyramidal cells (hereafter, pyramidal cells) exhibited a wide range of task-related activity in relation to cortical position (12 (including 3 identified) hold-related, 7 (including 4 identified) pre-movement, 38 (including 14 identified) movement, 6 (including 3 identified) movement-off, 4 (including 3 identified) post-movement and 3 (including 2 identified) non–task-related neurons; **Fig. 4b**), suggesting that there is a sequence of concurrent multi-layer integration (**Fig. 1e**), rather than a layer-by-layer conversion for sequential motor phases. In contrast with the diverse pyramidal-cell activity, all 16 (9 identified) task-related fast-spiking interneurons found in layers 2–6 exhibited only movement activity (χ^2 test, $P < 0.001$ between pyramidal cells and interneurons; **Fig. 4b**). Pyramidal cells and fast-spiking interneurons with movement activity were identified in all of layers 2/3, 4, 5 and 6. Thus, juxtacellular recordings revealed the multi-layer activation and the different functional diversity of pyramidal cells and fast-spiking interneurons.

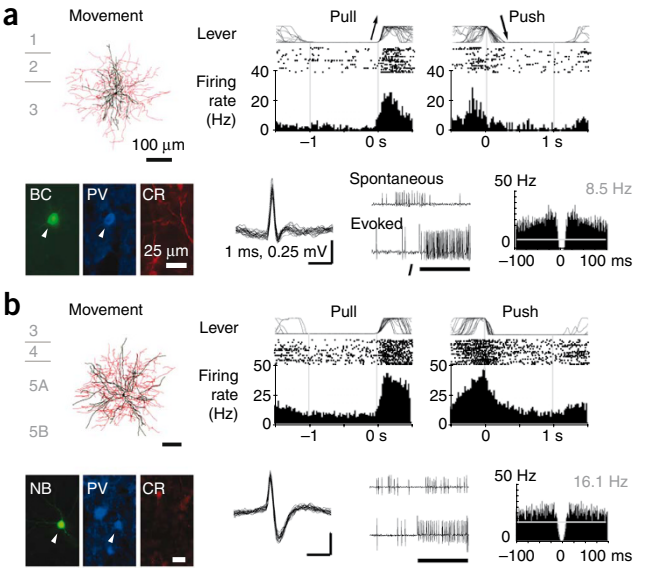

Figure 3 Movement-associated activation in identified fast-spiking interneurons. (**a**,**b**) Fast-spiking interneurons in layer 3 (**a**) and layer 5A (**b**) showing increased activity with pull movement (movement activity). Note that these biocytin (BC)- or Neurobiotin (NB)-visualized neurons (arrowheads) expressed parvalbumin (PV), a fast-spiking interneuron–specific marker, but not calretinin (CR), a marker of non–fast-spiking interneurons. They exhibited a higher evoked firing rate with a narrower spike width than pyramidal cells, which is characteristic of fast-spiking interneurons.

Activity properties of pyramidal cells and interneurons

The juxtacellularly recorded pyramidal cells had significantly lower rates of ongoing activity in superficial cortical layers (depth of <800 µm) than in deeper layers (superficial: 5.1 ± 6.6 Hz, n = 32; deep: 8.9 ± 7.3 Hz, n = 38; $P < 0.03$; identified layer 2/3: 2.2 ± 2.6 Hz, n = 6; identified layers 5–6: 9.4 ± 8.6 Hz, n = 21; $P < 0.003$; t test; **Fig. 5** and **Supplementary Figs. 6** and **7**). Similarly, the fast-spiking interneurons fired at lower rates in superficial layers than in deep layers, although the difference was not substantial (**Supplementary Fig. 7**). Moreover, baseline activity in the lever-hold period was much lower in regular-spiking neurons (multiunit; **Supplementary Fig. 7**) and pyramidal cells (juxtacellular; **Supplementary Fig. 7**) than in fast-spiking interneurons (except for one pre-movement and one post-movement neuron in multiunit analysis). Notably, baseline activity was much higher in movement-off pyramidal cells than in movement pyramidal cells, indicating that the movement-off activity was not inactivation of the movement activity in a nonpreferred direction (multiunit: movement, 3.2 ± 3.4 Hz; movement-off, 9.6 ± 7.4 Hz; t test, $P < 0.001$; juxtacellular: movement, 5.1 ± 6.5 Hz; movement-off, 20.1 ± 10.0 Hz; $P < 0.001$; identified movement, 7.5 ± 8.0 Hz; identified movement-off, 22.3 ± 11.5 Hz; $P < 0.02$).

The temporal profile of movement activity in fast-spiking interneurons (multiunit, n = 11; juxtacellular, n = 16) was parallel with, or slightly slower than, that of regular-spiking neurons (multiunit, n = 25) or pyramidal cells (juxtacellular, n = 28) (**Fig. 5a**). The peak latency of fast-spiking interneurons was delayed relative to pyramidal cells (fast-spiking, 96.3 ± 40.1 ms; pyramidal, 39.3 ± 50.6 ms; t test, $P < 0.001$; identified fast-spiking, 113.3 ± 43.6 ms, n = 9; identified pyramidal, 16.4 ± 39.8 ms, n = 11; t test, $P < 0.001$; **Fig. 5b**). *In vitro* experiments have suggested that motor information flows from a superficial-layer loop to a deep-layer loop in cortical microcircuits[16]. Pyramidal cell and fast-spiking interneuron latencies, however, did not differ on the basis of layer in our self-paced movement condition (superficial versus deep; $P > 0.3$ and $P > 0.2$, respectively).

There were differences in the direction coding of pyramidal cells and fast-spiking interneurons, although pull and push movements were not strictly equivalent in our simple task condition. Consistent with previous studies[27,32], movement activity was reduced from baseline levels (in lever-hold period) during the nonpreferred movement (push or pull) in 16 of 51 regular-spiking neurons and 15 of 38 pyramidal cells (**Figs. 2c** and **5c** and **Supplementary Fig. 6**). However, only 2 of 13 (multiunit) and 0 of 16 (juxtacellular) fast-spiking interneurons with movement activity exhibited such antagonistic inactivation (**Figs. 3** and **5c**). Thus, the direction specificity of fast-spiking interneurons was substantial, but was significantly weaker than that of regular-spiking neurons or pyramidal cells (multiunit: regular-spiking, 0.50 ± 0.29 for direction specificity; fast-spiking, 0.21 ± 0.16; t test, $P < 0.001$; juxtacellular: pyramidal cells, 0.48 ± 0.29; interneurons 0.31 ± 0.19; $P < 0.025$; identified pyramidal cells, 0.57 ± 0.35; identified interneurons, 0.35 ± 0.22; $P = 0.11$; **Fig. 5c–e**). Furthermore, multiunit recordings at identical electrode sites revealed that 71% of regular spiking–regular spiking neuron pairs with movement activity had similar direction specificity (relative direction specificity, 0.18 ± 0.55, n = 118 pairs, t test, $P < 0.001$; **Fig. 5d**), whereas the direction specificity of fast-spiking interneurons seemed to be independent of nearby regular-spiking neurons (−0.06 ± 0.59, n = 20, $P > 0.6$). This

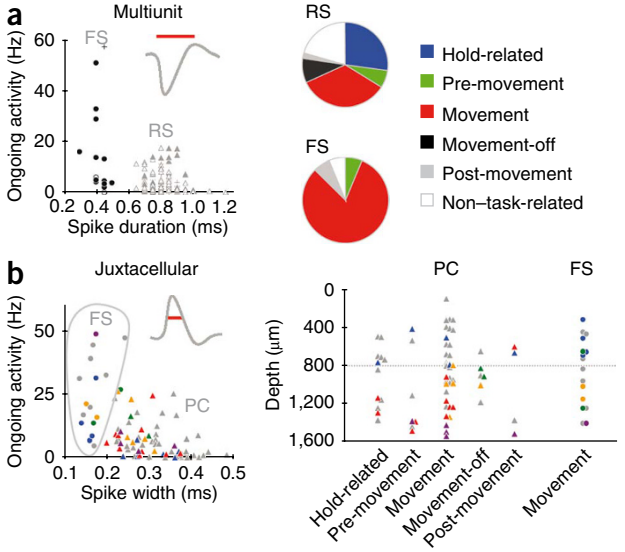

Figure 4 Contrasting functional diversity between pyramidal cells and fast-spiking interneurons. (**a**) Functionally different groups of regular-spiking (RS) and fast-spiking (FS) neurons in the multiunit analysis. Left, classification of isolated units as regular-spiking (gray) and fast-spiking (black) by spike duration (red bar). Filled symbols represent movement activity, open symbols represent other task-related activity and pluses represent non–task-related activity. Right, population ratios of functionally different neuron groups for regular-spiking and fast-spiking neurons. (**b**) Functionally different groups of pyramidal cells (PCs) and fast-spiking interneurons in the juxtacellular analysis. Left, distribution of identified pyramidal cells (colored triangles) and fast-spiking interneurons (colored circles) and the classification of unidentified neurons as putative pyramidal cells (gray triangles) and putative fast-spiking interneurons (gray circles) by spike width (red bar) and ongoing firing rate. Right, the cortical distribution of functionally different neuron groups. Blue symbols represent layer 2/3, green represents layer 4, orange represents layer 5A, red represents layer 5B and purple represents layer 6.

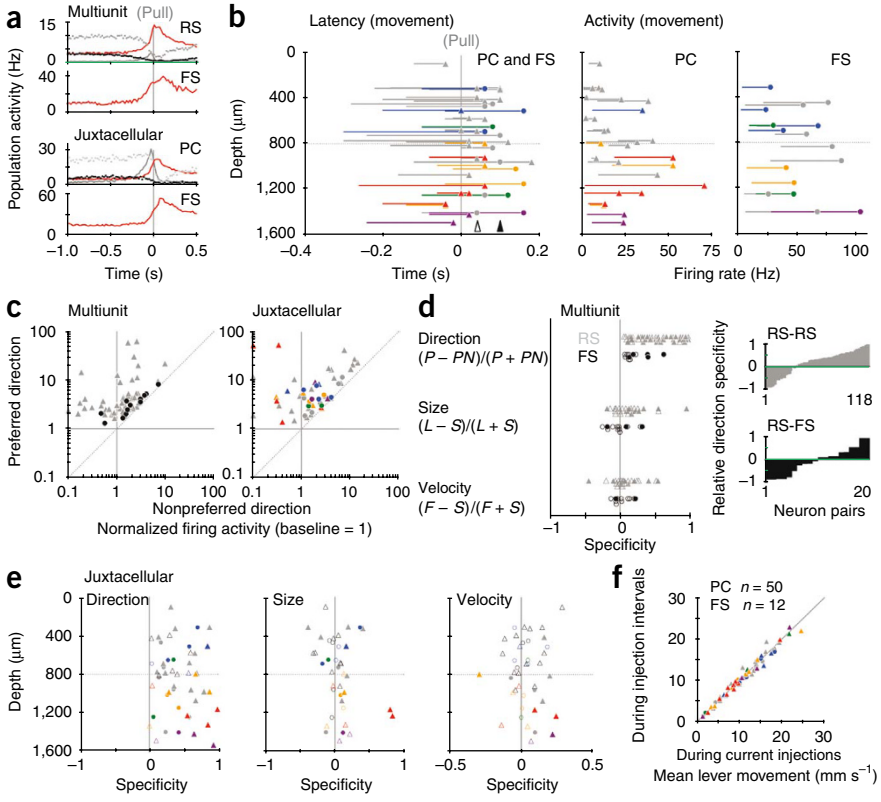

Figure 5 Time course and specificity in pyramidal cells and fast-spiking interneurons with movement activity. (**a**) Population (averaged) firing activity for functionally different neuron groups (black line indicates hold-related activity, gray line indicates pre-movement, red line indicates movement and the gray dotted line indicates movement-off) aligned with pull onset (0 s) in multiunit and juxtacellular recordings. (**b**) Left, cortical position and onset (left edge) to peak latency (symbol) of movement activity for individual neurons. Symbols are as described in **Figure 4**. Open and filled arrowheads indicate mean peak latency in pyramidal cells and fast-spiking interneurons, respectively. Right, cortical position and baseline (left edge) to peak activity (symbol) of movement activity for individual neurons. (**c**) Normalized changes in movement activity in preferred and nonpreferred directions (pull/push; normalized with baseline firing rate) in multiunit and juxtacellular analyses. (**d**) Left, specificities of movement activity for direction (upper), size (middle) and velocity (lower) in regular-spiking (n = 51, 25 and 25 available for analysis, respectively) and fast-spiking (n = 13, 13 and 11) neurons from multiunit recordings. Filled symbols denote significance ($P < 0.05$) and open symbols are nonsignificant ($P > 0.05$) in **d** and **e**. Right, coherence of direction specificity in local regular spiking–regular spiking and regular spiking–fast spiking neuron pairs with movement activity. Positive and negative values indicate the same and opposite preferred directions in individual neuron pairs, respectively. See the Online Methods for details. (**e**) The cortical position and specificities of movement activity for direction (left), size (middle) and velocity (right) in pyramidal cells (n = 33, 25 and 27, respectively) and fast-spiking interneurons (n = 16, 14 and 14) from juxtacellular recordings. (**f**) There were no effects of juxtacelluar current injection into single pyramidal cells (n = 50) or interneurons (n = 12) on lever-movement performance.

suggested that fast-spiking interneurons might not modulate selective movement activity of regular-spiking neurons.

Motor cortex neurons principally encode the force[33] and direction[32] of movement, but their activity is often modulated by the size and velocity of movement[34,35]. Some pyramidal cells and fast-spiking interneurons with movement activity conveyed modulatory information on the size or velocity of movement in our constant force condition (**Fig. 5d**,**e**). The size (multiunit, $P > 0.06$; juxtacellular, $P > 0.3$) and velocity (multiunit, $P > 0.5$; juxtacellular, $P > 0.5$) specificities of fast-spiking interneurons did not differ significantly from those of regular-spiking neurons or pyramidal cells. Furthermore, we found no significant differences in the above specificities between superficial and deep layers (size, $P > 0.8$; velocity, $P > 0.9$). Unlike in the whisker motor cortex[36], juxtacellular current injection into single neurons did not affect the performance of forelimb movements (**Fig. 5f**).

Synaptic interactions among functionally different neurons

To examine the network machinery bridging the sequential motor phases, we searched for excitatory synaptic interactions between neuron pairs[28–31] in the multiunit (n = 166) and juxtacellular (n = 30) data pool (total of 872 pairs in 22 rats). We examined putatively monosynaptic excitatory connectivity from a hold-related to a movement regular-spiking neuron and from a pre-movement regular-spiking neuron to a movement fast-spiking neuron, respectively, along the flow of motor information (**Fig. 6a**,**b**). We created cross-correlation histograms and found clear, several-fold, single peaks around 1.5 ms after presynaptic neuron firing. Unexpectedly, a pre-movement regular-spiking neuron excited not only a movement fast-spiking interneuron, but also a hold-related regular-spiking neuron against the motor information flow (**Fig. 6c**). This result suggests that the network machinery for voluntary movement expression is not a simple feedforward network for processing sequential motor phases. The single peak observed in the cross-correlation histogram (asymmetric, short latency with small jitter, and statistically large amplitude) most likely represented monosynaptic excitation between two distinct neurons (see refs. 28, 30 and 31), as the spike waveform and amplitude ratio in raw and averaged traces were completely different between the two neurons, the peak latency (typically, 1–2 ms) was too fast to be burst-spiking of one regular-spiking neuron or a polysynaptic response and too late to be gap junction–mediated synchronization, and the peak position was too tightly asymmetric to be common-input response. In addition, spike clusters including burst activity from one neuron had been concatenated into a single spike cluster in advance and the single peak was preserved after all overlapping outlier spikes were excluded in a two-dimensional plane out of 17 spike-feature parameters (**Supplementary Fig. 8**). The single peak disappeared after shuffling trials in the triggering neuron (**Supplementary Fig. 8**). However, we cannot exclude the possibility that one presynaptic neuron commonly activated two postsynaptic neurons with different synaptic delays.

We obtained 19 putatively monosynaptic excitatory connections out of the 872 possible neuron pairs. We did not examine inhibitory connections and suspected common-input responses with no delay, as spikes can decrease or increase over the 0-ms bin in a cross-correlogram

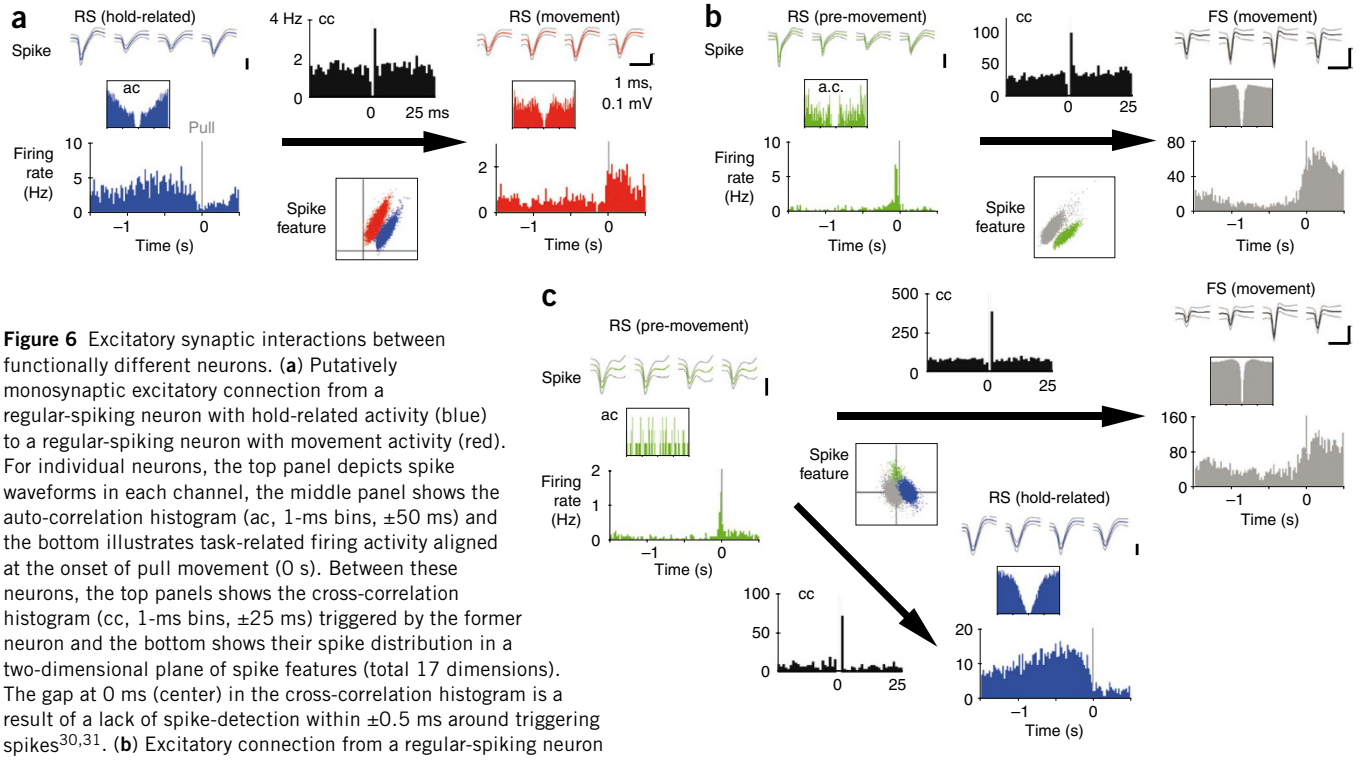

Figure 6 Excitatory synaptic interactions between functionally different neurons. (**a**) Putatively monosynaptic excitatory connection from a regular-spiking neuron with hold-related activity (blue) to a regular-spiking neuron with movement activity (red). For individual neurons, the top panel depicts spike waveforms in each channel, the middle panel shows the auto-correlation histogram (ac, 1-ms bins, ±50 ms) and the bottom illustrates task-related firing activity aligned at the onset of pull movement (0 s). Between these neurons, the top panels shows the cross-correlation histogram (cc, 1-ms bins, ±25 ms) triggered by the former neuron and the bottom shows their spike distribution in a two-dimensional plane of spike features (total 17 dimensions). The gap at 0 ms (center) in the cross-correlation histogram is a result of a lack of spike-detection within ±0.5 ms around triggering spikes[30,31]. (**b**) Excitatory connection from a regular-spiking neuron with pre-movement activity (green) to a fast-spiking interneuron with movement activity (gray). (**c**) Excitatory connections from a regular-spiking neuron with pre-movement activity (green) to a fast-spiking interneuron with movement activity (gray) and to a regular-spiking neuron with hold-related activity (blue).

by other unknown mechanisms. Notably, we frequently found synaptic interactions between presynaptic regular-spiking neurons and postsynaptic neurons engaging in various functional activities, irrespective of the temporal order expected from their functional activities (for example, pre-movement to hold-related). In particular, pre-movement regular-spiking neurons, which might participate in motor initiation, excited similar pre-movement regular-spiking neurons as well as regular-spiking and fast-spiking neurons with different functional activities (three pre-movement, four hold-related and one movement regular-spiking neurons, three movement fast-spiking neurons; **Supplementary Fig. 8**). Although more putative monosynaptic connections must be examined for rigorous quantification, many of the excitatory connections originated from the small population of pre-movement neurons (see **Fig. 4**). In at least 12 of the 19 pairs, the synaptic excitation between functionally different neurons was effective during the task performance (**Supplementary Fig. 8**). The excitatory synaptic communications between functionally different groups of cortical neurons may integrate motor information relevant to self-initiated voluntary movement.

DISCUSSION

Multilayer activation for sequential motor phases

Our behavioral and electrophysiological approach revealed that excitatory pyramidal cells in multiple layers of the motor cortex have temporally different activations, which probably correspond to sequential motor phases, that most of the inhibitory fast-spiking interneurons were activated during movement expression, and that synchronous spike responses were evoked between functionally different neurons in self-initiation of voluntary forelimb movement.

Several *in vitro* studies have predicted a directional signaling pathway through particular layers of motor cortex[14–16]. An *in vivo* study reported that putative pyramidal cells in layer 5, but not in layers 2/3 or 6, were activated on a specific phase of the locomotion cycle[19]. However, our findings of simultaneous multilayer activation in juxtacellular visualization (**Figs. 4** and **5**) exclude the possibility that motor information may be converted for sequential motor phases layer by layer. Some striatal neurons had temporally different activations that were similar to those of cortical neurons during the same forelimb movement (data not shown). Thus, the multilayer activation of pyramidal cells might result from global and concurrent interactions with other cortical areas, as well as subcortical structures for each motor phase. How the information for each motor phase flows from one layer to another and how non–fast-spiking interneurons that were not characterized here may be recruited for coordinating this flow remain unknown.

Command-shaping function of fast-spiking interneurons

Inhibitory fast-spiking interneurons, typically morphological basket cells or chandelier cells making axo-somatic or axo-axonic synapses, may effectively gate spike outputs from the pyramidal cells[18]. In fact, putative fast-spiking interneurons of the rabbit motor cortex are activated on the opposite phase to activation of putative pyramidal cells in every cycle of locomotion, which consists of continuous and complex limb movements under subcortical pattern controls[19]. In contrast, our results from the juxtacellular analysis indicate that the majority of identified fast-spiking interneurons probably participate in an on-going modulation of command-like activity of pyramidal cells during the execution of a single voluntary movement (**Figs. 4** and **5**). Notably, the absence of fast-spiking interneurons with movement-off activity excludes the possibility of intracortical gating of motor command.

Several recent studies have suggested that excitatory and inhibitory inputs should be balanced to regulate spontaneous or sensory-evoked neuronal activity in sensory cortex neurons under anesthesia[37,38].

There is a balance between inhibitory and excitatory synaptic inputs in auditory[37] and somatosensory[38] cortex neurons, and inhibitory synaptic inputs always succeed excitatory synaptic inputs, making output timing more precise. Fast-spiking interneurons of the motor cortex were also activated slightly after command-like activation of pyramidal cells in behaving rats (**Fig. 5a**,**b**), suggesting that balanced and delayed inhibition may achieve temporal sharpening of motor command. Moreover, fast-spiking interneurons with movement activity might suppress other functional activities such as hold-related activity during motor execution.

The activity of fast-spiking interneurons was less specific to movement direction than that of regular-spiking neurons and was independent of the preferred direction of neighboring regular-spiking neurons in the rat motor cortex (**Fig. 5c–e**). Thus, the balanced inhibition might work effectively at the surround as well as the center of intended movement, presumably to sharpen the direction specificity of pyramidal cells through the so-called iceberg effect[37]. In fact, a pharmacological blockade of GABAergic inhibition in the primate motor cortex increases the phasic discharge activity in a preferred direction and decreases its directionality[39]. Alternatively, fast-spiking interneurons activated by movement pyramidal cells might accomplish recurrent inhibition of other pyramidal cell activity to suppress competing (unnecessary) movements. In the primate motor cortex, where putative fast-spiking interneurons show directional tuning properties[27], the cortico-spinal pyramidal cells elicit disynaptic inhibitory responses in neighboring neurons[40,41]. However, putative fast-spiking interneurons and nearby putative pyramidal cells in the primate prefrontal cortex have increased activation in the same or in the opposite preferred direction, depending on task conditions[29,42,43]. Although fast-spiking interneurons probably underlie temporal or spatial 'shaping' of motor command with a subgroup of pyramidal cells across all layers of motor cortex, an intracellular measurement of excitatory and inhibitory synaptic inputs[37,38] will be needed to conclude whether the fast-spiking interneurons are engaged in balanced inhibition, recurrent inhibition or both.

Synaptic communications in cortical microcircuits

How do functionally different neurons integrate motor information to express self-initiated voluntary movement? The spiking of a single motor-cortex neuron evokes an excitatory or inhibitory postsynaptic potential in neighboring neurons in awake monkeys[44]. Our multiunit recording also revealed putatively monosynaptic connectivity between pairs of regular-spiking neurons and between regular-spiking and fast-spiking neurons in the deep layers of the rat motor cortex (**Fig. 6**). Notably, monosynaptic excitation was detected in regular spiking–regular spiking and regular spiking–fast spiking neuron pairs with different functional activities, unlike in the primate prefrontal cortex, where the phasic activation of neuron pairs showing excitatory communications does not have a large temporal difference during a working-memory task[29]. As the direction of synaptic excitation did not always coincide with the temporal order of functional activity (for example, pre-movement to hold-related in **Fig. 6c**), serial motor phases are unlikely to be relayed solely by the intramicrocircuit synaptic interaction. It is possible that specific cortico-cortical pathways and cortico-subcortical loops also participate in this relay. We found that pre-movement regular-spiking neurons excited excitatory and inhibitory neurons with similar or different functional activity (**Fig. 6b**,**c** and **Supplementary Fig. 8**). A recurrent network formed by similar pre-movement regular-spiking neurons may accomplish temporal integration[45] of motor signals to decide the timing of self-initiated movement. Our juxtacellular recordings revealed that some of the pre-movement regular-spiking neurons sent axonal projections to subcortical structures (**Fig. 2b**,**f** and **Supplementary Fig. 6**). It is possible that these pre-movement regular-spiking neurons are important for intracortical and cortico-subcortical integration of motor information to coordinate sequential motor phases.

Alternatively, the short-latency peak that appeared in our cross-correlogram may arise from a common excitatory drive on the two recorded neurons with different delays. In this case, spike correlations do not represent direct synaptic interactions between functionally different neurons, but may represent the recruitment of functionally heterogeneous neurons by a presynaptic neuron through highly reliable synaptic excitation. This possibility cannot be excluded by the present cross-correlation analysis. In either of the above cases, the microcircuit of motor cortex is suggested to process motor information with a specifically designed neuronal wiring between different functional cell assemblies.

Technical advantages and functional implications

Juxtacellular recording enabled us to examine accurate spike events and morphological features of a single neuron in arbitrary layer of the cerebral cortex[20–22] and in many subcortical structures[23,24] (**Supplementary Fig. 6**) *in vivo*. The access to deep brain structures is a technical advantage over calcium-imaging with multi-photon laser-scanning microscopy. Although juxtacellular recording has been conducted in anesthetized[20–23] or sleeping/waking[24] animals, the juxtacellular identification of naturally spiking neurons has not been attempted in actively task-performing animals, to the best of our knowledge (see ref. 46 for stimulation). For reliable visual discrimination, we could obtain only one (or a few) juxtacellularly recorded neuron(s) in each rat, which had to be killed within 24 h[20]. Therefore, juxtacellular experiments focusing on cognitive or motor functions require a substantial number of head-restraint animals performing an operant behavioral task. However, it is usually difficult and time consuming to train head-restraint rodents, unlike primates[47], to learn an operant forelimb-movement task. Our multi-rat task-training system markedly improved the efficiency of preparing task-performing rats for final experiments (**Supplementary Figs. 1–3** and **Supplementary Videos 1** and **2**). This method should be also useful for other physiological measurements, such as whole-cell patch-clamp recordings[36], voltage-sensitive dye imaging[48] and calcium-imaging with multi-photon laser-scanning microscopy[49] in head-restraint rodents.

Using the experimental approach, these results shed light on the intracortical mechanism of motor-command generation in the expression of voluntary movements via circuit level analysis. Our results led to the hypothesis of multilayer simultaneous processing for sequential motor phases. In this hypothesis, a group of pyramidal cells in superficial and deep layers may become gradually active to prepare for an intended movement, whereas fast-spiking interneurons do not affect the preparatory activity during the stationary behavior. Once additional pyramidal cells begin to discharge, they self-amplify the transient signal by exciting functionally similar pyramidal cells to initiate the movement. The reverberating excitation may decide the timing as well as the direction of movement. Subsequently, the major population of pyramidal cells across all layers generates an output command to execute the movement and fast-spiking interneurons are coactivated to shape the motor command via balanced inhibition or recurrent inhibition.

METHODS

Methods and any associated references are available in the online version of the paper at http://www.nature.com/natureneuroscience/.

Note: Supplementary information is available on the Nature Neuroscience website.

ACKNOWLEDGMENTS

We thank G. Buzsáki and J. Tanji for helpful comments and discussion, M. Fujii, K. Ishii, M. Kobayashi, R. Nakatomi and S. Tanaka for technical assistance, and K. O'hara for developing the multi-rat task-training system. This work was supported by the institutional research grants from RIKEN (T.F.) and by Grants-in-Aid for Scientific Research from Ministry of Education, Culture, Sports, Science and Technology (18019041 and 18700386 to Y.I. and 40218871 to T.F.).

AUTHOR CONTRIBUTIONS

Y.I. designed the experiments. Y.I., R.H. and H.A. performed the experiments. Y.I. and T.T. analyzed the data. Y.I. and T.F. wrote the paper.

Published online at http://www.nature.com/natureneuroscience/.
Reprints and permissions information is available online at http://www.nature.com/reprintsandpermissions/.

1. Deecke, L., Scheid, P. & Kornhuber, H.H. Distribution of readiness potential, pre-motion positivity, and motor potential of the human cerebral cortex preceding voluntary finger movements. *Exp. Brain Res.* **7**, 158–168 (1969).
2. Hashimoto, S., Gemba, H. & Sasaki, K. Premovement slow cortical potentials and required muscle force in self-paced hand movements in the monkey. *Brain Res.* **197**, 415–423 (1980).
3. Tanji, J. & Evarts, E.V. Anticipatory activity of motor cortex neurons in relation to direction of an intended movement. *J. Neurophysiol.* **39**, 1062–1068 (1976).
4. Okano, K. & Tanji, J. Neuronal activities in the primate motor fields of the agranular frontal cortex preceding visually triggered and self-paced movement. *Exp. Brain Res.* **66**, 155–166 (1987).
5. Hyland, B. Neural activity related to reaching and grasping in rostral and caudal regions of rat motor cortex. *Behav. Brain Res.* **94**, 255–269 (1998).
6. Chapin, J.K., Moxon, K.A., Markowitz, R.S. & Nicolelis, M.A.L. Real-time control of a robot arm using simultaneously recorded neurons in the motor cortex. *Nat. Neurosci.* **2**, 664–670 (1999).
7. Laubach, M., Wessberg, J. & Nicolelis, M.A.L. Cortical ensemble activity increasingly predicts behaviour outcomes during learning of a motor task. *Nature* **405**, 567–571 (2000).
8. Bauswein, E., Fromm, C. & Preuss, A. Corticostriatal cells in comparison with pyramidal tract neurons: contrasting properties in the behaving monkey. *Brain Res.* **493**, 198–203 (1989).
9. Turner, R.S. & DeLong, M.R. Corticostriatal activity in primary motor cortex of the macaque. *J. Neurosci.* **20**, 7096–7108 (2000).
10. Fromm, C. Contrasting properties of pyramidal tract neurons located in the precentral or postcentral areas and of corticorubral neurons in the behaving monkey. *Adv. Neurol.* **39**, 329–345 (1983).
11. Donoghue, J.P. & Wise, S.P. The motor cortex of the rat: cytoarchitecture and microstimulation mapping. *J. Comp. Neurol.* **212**, 76–88 (1982).
12. Rouiller, E.M., Moret, V. & Liang, F. Comparison of the connectional properties of the two forelimb areas of the rat sensorimotor cortex: support for the presence of a premotor or supplementary motor cortical area. Somatosens. *Mot. Res.* **10**, 269–289 (1993).
13. Brecht, M. *et al.* Organization of rat vibrissa motor cortex and adjacent areas according to cytoarchitectonics, microstimulation and intracellular stimulation of identified cells. *J. Comp. Neurol.* **479**, 360–373 (2004).
14. Cho, R.-H., Segawa, S., Mizuno, A. & Kaneko, T. Intracellularly labeled pyramidal neurons in the cortical areas projecting to the spinal cord. I. Electrophysiological properties of pyramidal neurons. *Neurosci. Res.* **50**, 381–394 (2004).
15. Cho, R.-H. *et al.* Intracellularly labeled pyramidal neurons in the cortical areas projecting to the spinal cord. II. Intra- and juxta-columnar projection of pyramidal neurons to corticospinal neurons. *Neurosci. Res.* **50**, 395–410 (2004).
16. Weiler, N. *et al.* Top-down laminar organization of the excitatory network in motor cortex. *Nat. Neurosci.* **11**, 360–366 (2008).
17. Cauli, B. *et al.* Molecular and physiological diversity of cortical nonpyramidal cells. *J. Neurosci.* **17**, 3894–3906 (1997).
18. Markram, H. *et al.* Interneurons of the neocortical inhibitory system. *Nat. Rev. Neurosci.* **5**, 793–807 (2004).
19. Beloozerova, I.N., Sirota, M.G. & Swadlow, H.A. Activity of different classes of neurons of the motor cortex during locomotion. *J. Neurosci.* **23**, 1087–1097 (2003).
20. Pinault, D. A novel single-cell staining procedure performed *in vivo* under electrophysiological control: morpho-functional features of juxtacellularly labeled thalamic cells and other central neurons with biocytin or Neurobiotin. *J. Neurosci. Methods* **65**, 113–136 (1996).
21. Klausberger, T. *et al.* Brain state– and cell type–specific firing of hippocampal interneurons *in vivo*. *Nature* **421**, 844–848 (2003).
22. de Kock, C.P.J., Bruno, R.M., Spors, H. & Sakmann, B. Layer- and cell type–specific suprathreshold stimulus representation in rat primary somatosensory cortex. *J. Physiol. (Lond.)* **581**, 139–154 (2007).
23. Mallet, N., Ballion, B., Le Moine, C. & Gonon, F. Cortical inputs and GABA interneurons imbalance projection neurons in the striatum of parkinsonian rats. *J. Neurosci.* **26**, 3875–3884 (2006).
24. Lee, M.G., Manns, I.D., Alonso, A. & Jones, B.E. Sleep-wake related discharge properties of basal forebrain neurons recorded with micropipettes in head-fixed rats. *J. Neurophysiol.* **92**, 1182–1198 (2004).
25. Harris, K.D. *et al.* Accuracy of tetrode spike separation as determined by simultaneous intracellular and extracellular measurements. *J. Neurophysiol.* **84**, 401–414 (2000).
26. Isomura, Y. *et al.* Integration and segregation of activity in entorhinal-hippocampal subregions by neocortical slow oscillations. *Neuron* **52**, 871–882 (2006).
27. Merchant, H., Naselaris, T. & Georgopoulos, A.P. Dynamic sculpting of directional tuning in the primate motor cortex during three-dimensional reaching. *J. Neurosci.* **28**, 9164–9172 (2008).
28. Csicsvari, J., Hirase, H., Czurko, A. & Buzsáki, G. Reliability and state dependence of pyramidal cell-interneuron synapses in the hippocampus: an ensemble approach in the behaving rat. *Neuron* **21**, 179–189 (1998).
29. Constantinidis, C., Williams, G.V. & Goldman-Rakic, P.S. A role for inhibition in shaping the temporal flow of information in prefrontal cortex. *Nat. Neurosci.* **5**, 175–180 (2002).
30. Barthó, P. *et al.* Characterization of neocortical principal cells and interneurons by network interactions and extracellular features. *J. Neurophysiol.* **92**, 600–608 (2004).
31. Sirota, A. *et al.* Entrainment of neocortical neurons and gamma oscillations by the hippocampal theta rhythm. *Neuron* **60**, 683–697 (2008).
32. Georgopoulos, A.P., Kalaska, J.F., Caminiti, R. & Massey, J.T. On the relations between the direction of two-dimensional arm movements and cell discharge in primate motor cortex. *J. Neurosci.* **2**, 1527–1537 (1982).
33. Evarts, E.V. Relation of pyramidal tract activity to force exerted during voluntary movement. *J. Neurophysiol.* **31**, 14–27 (1968).
34. Humphrey, D.R., Schmidt, E.M. & Thompson, W.D. Predicting measures of motor performance from multiple cortical spike trains. *Science* **170**, 758–762 (1970).
35. Fromm, C. & Evarts, E.V. Relation of size and activity of motor cortex pyramidal tract neurons during skilled movements in the monkey. *J. Neurosci.* **1**, 453–460 (1981).
36. Brecht, M., Schneider, M., Sakmann, B. & Margrie, T.W. Whisker movements evoked by stimulation of single pyramidal cells in rat motor cortex. *Nature* **427**, 704–710 (2004).
37. Wehr, M. & Zador, A.M. Balanced inhibition underlies tuning and sharpens spike timing in auditory cortex. *Nature* **426**, 442–446 (2003).
38. Okun, M. & Lampl, I. Instantaneous correlation of excitation and inhibition during ongoing and sensory-evoked activities. *Nat. Neurosci.* **11**, 535–537 (2008).
39. Matsumura, M., Sawaguchi, T. & Kubota, K. GABAergic inhibition of neuronal activity in the primate motor and premotor cortex during voluntary movement. *J. Neurophysiol.* **68**, 692–702 (1992).
40. Stefanis, C. & Jasper, H. Recurrent collateral inhibition in pyramidal tract neurons. *J. Neurophysiol.* **27**, 855–877 (1964).
41. Georgopoulos, A.P. & Stefanis, C.N. Local shaping of function in the motor cortex: motor contrast, directional tuning. *Brain Res. Rev.* **55**, 383–389 (2007).
42. Wilson, F.A.W., Scalaidhe, Ó.S.P. & Goldman-Rakic, P.S. Functional synergism between putative γ-aminobutyrate–containing neurons and pyramidal neurons in prefrontal cortex. *Proc. Natl. Acad. Sci. USA* **91**, 4009–4013 (1994).
43. Rao, S.G., Williams, G.V. & Goldman-Rakic, P.S. Isodirectional tuning of adjacent interneurons and pyramidal cells during working memory: evidence for microcolumnar organization in PFC. *J. Neurophysiol.* **81**, 1903–1916 (1999).
44. Matsumura, M. *et al.* Synaptic interactions between primate precentral cortex neurons revealed by spike-triggered averaging of intracellular membrane potentials *in vivo*. *J. Neurosci.* **16**, 7757–7767 (1996).
45. Okamoto, H. & Fukai, T. Recurrent network models for perfect temporal integration of fluctuating correlated inputs. *PLoS Comput. Biol.* **5**, e1000404 (2009).
46. Houweling, A.R. & Brecht, M. Behavioural report of single neuron stimulation in somatosensory cortex. *Nature* **451**, 65–68 (2008).
47. Isomura, Y. *et al.* Neural coding of "attention for action" and "response selection" in primate anterior cingulate cortex. *J. Neurosci.* **23**, 8002–8012 (2003).
48. Ferezou, I. *et al.* Spatiotemporal dynamics of cortical sensorimotor integration in behaving mice. *Neuron* **56**, 907–923 (2007).
49. Dombeck, D.A. *et al.* Imaging large-scale neural activity with cellular resolution in awake, mobile mice. *Neuron* **56**, 43–57 (2007).

ONLINE METHODS

Animal preparation. All experiments were carried out in accordance with the Animal Experiment Plan approved by the Animal Experiment Committee of RIKEN. Adult Long-Evans rats (150–250 g, male, Japan SLC) were handled briefly and adapted to a stainless steel cylinder in their home cage (**Fig. 1a** and **Supplementary Fig. 1**). A lightweight, sliding head attachment (custom-made by Narishige Co.) was surgically attached to the skull and reference electrodes were implanted above the cerebellum under 2% isoflurane (vol/vol) anesthesia. After recovering from surgery, the rats were deprived of drinking water in their home cages, although food was available *ad libitum*. Sufficient water was provided as a reward for task performance in the laboratory. If necessary, the rats were provided an agar block (containing 15 ml of water) to maintain over 80% of their body weight.

Behavioral training. To efficiently train head-restrained rats to repeat regular movements, we developed a multi-rat task-training system (now available from O'hara & Co.), which consisted of six training boxes that were each controlled by a computer (**Supplementary Fig. 2**). Each animal was placed in a separate training box and trained to perform the voluntary (self-paced) forelimb-movement task while being head-restrained for 2–2.5 h a day (8 training days in 2 weeks; **Supplementary Fig. 3**). At the endpoint of this task learning, the rat spontaneously started each trial by pushing a constant-torque lever and holding the lever for more than 1 s with the right forelimb. If the rat pulled the lever for more than 60% of a full lever-shift (12 mm), then the rat received a drop of 0.1% saccharin water (wt/vol, 0.01–0.02 ml) in their mouth from a spout connected to a syringe pump after a 0.2-s delay. The lever position was continuously monitored by the task-control computer with an 8-bit encoder and forelimb motion was monitored with an infrared video camera. A high-tone sound (11 kHz) was accompanied by the reward delivery and a low-tone sound (3 kHz) was emitted after a task failure. During the early training stage, the rats were rewarded whenever they moved the lever, regardless of the amount of movement. Lever shift and hold-time requirements for reward acquisition progressively increased during the first week. Initially, rats had to support their body by seizing a side handrail with their left forelimb; however, they were permitted to use an optional armrest during the second week. To start task and recording experiments simultaneously, rats experienced a waiting period of 1 h with the lever locked before every task learning session in the second week.

Once the rats completed the operant task learning, they were transferred to the recording room to practice performing the same task in a novel environment for the final behavioral and electrophysiological experiment (**Supplementary Fig. 4**). The following day, the rats were subjected to a second surgery under isoflurane anesthesia and a tiny hole in the skull and dura matter were made above the left forelimb area (1.0 mm anterior, 2.5–3.0 mm lateral of bregma). The hole was covered with silicon sealant until the recording experiment commenced.

Electrophysiological recordings. We obtained juxtacellular recordings[20] from single neuron(s) in the left forelimb area of individual animals behaving in the task-control system 1 d after the second surgery. The glass electrode (BF150-75-10, Sutter Instrument) was prepared by a laser puller (P-2000, Sutter Instrument) and a blunt tip was created (**Supplementary Fig. 5**). The electrode was filled with 2% biocytin (wt/vol; Sigma-Aldrich) in 0.5 M NaCl or 2% Neurobiotin (wt/vol; Vector Laboratories) in 0.5 M KCl (12–24 MΩ). The electrode was inserted vertically into the forelimb area with a microdrive (LSS-8000 Inchworm, Burleigh Instrument) that was installed on a fine micromanipulator (1760-61, David Kopf Instruments) on a stereotaxic frame (SR-8N, Narishige). Juxtacellular signals were amplified with an intracellular amplifier (IR-283, Cygnus Tech) and sampled at 20 kHz (final gain of 1,000; band-pass filter, 300 Hz to 10 kHz) with a hard-disc recorder (DataMax II, R.C. Electronics). Subsequently, biocytin or Neurobiotin was electroporated into single recorded neurons with a positive current pulse (2–20 nA, 0.5-s duration, every 1 s, 10–45 min). The electrode depth was used to estimate the cortical position of identified and unidentified neurons ($r = 0.85$, $P < 0.001$; see **Supplementary Fig. 7**). Single neuron recordings were combined with extracellular multiunit recordings[25,26] from the same area through a wire tetrode or 16-channel silicon probe placed 1,200 μm deep (sampling, 20 kHz; final gain, 2,000; original band-pass filter, 0.5 Hz to 10 kHz). In preliminary experiments, EMG recordings[47] were obtained during task performance from the right upper forelimb and hindlimb through wire electrodes (**Fig. 1d**). To determine the coordinates of the forelimb area, we applied intracortical microstimulation (about −50 μA, 20 pulses at 500 Hz) to evoke selective EMG activity in the contralateral forelimb[47] under urethane anesthesia (**Supplementary Fig. 4**).

Histological staining. Under deep anesthesia, rats were killed by intracardial perfusion with cold saline followed by 4% paraformaldehyde (wt/vol) in 0.1 M phosphate buffer. Postfixed brains were sliced coronally into 50-μm-thick serial sections[26]. Biotin/Neurobiotin-loaded neurons were visualized with streptavidin-AlexaFluor488 (Molecular Probes) in combination with immunostaining for parvalbumin and calretinin (antibody to parvalbumin (MAB1572, Chemicon International) and antibody to calretinin (AB5054, Chemicon) followed by AlexaFluor350- and AlexaFluor594-conjugated secondary antibodies (Molecular Probes), respectively). After fluorescence microscopy, labeled neurons were further examined using the avidin-biotin–horseradish peroxidase complex (Vectstain Elite ABC, Vector) with diaminobenzidine and nickel[26]. Visualized neurons were reconstructed with camera lucida following counterstaining with Neutral Red.

Data analysis. Behavioral scores were compiled from trial-log files produced automatically by the task-control systems. Multiunit (and juxtacellular) recording data were processed to isolate spike events by the automatic spike-sorting program KlustaKwik using principal component analysis (17 feature dimensions for 4 channels; high-pass filter, 300 Hz; time resolution, 20 kHz; spike-detection interval, >0.5 ms). Next, the sorted spike clusters were combined, divided or discarded manually to refine single-neuron clusters by Klusters and NeuroScope[25,26,50]. The relationship of spike activity with behavioral performance was analyzed by MATLAB (MathWorks). The behavior-related spike activity was categorized into five temporally (functionally) different groups (**Fig. 5a**). Hold-related activity was a unimodal (increasing, decreasing or increasing to decreasing) activation during the lever-holding period. Pre-movement was a phasic activation starting less than 500 ms before the movement onset and falling down below the half peak at the movement onset. Movement was a phasic activation during the movement. Movement-off activity was an abrupt drop-off during the movement after constant tonic spiking in the intertrial-interval and lever-holding periods. Post-movement was a phasic activation showing a larger peak in the movement end–aligned histogram than the movement onset–aligned histogram. The phasic activation/inactivation contained at least three consecutive bins (20 ms) ±3 s.d. from the baseline activity (0.25–1 s before the movement onset); furthermore, these categorized activities were checked by a visual inspection. Ongoing activity was defined as the average firing rate (before juxtacellular current injection). The spike duration was the time from spike onset to the first positive peak and the spike width referred to the elapsed time above the half amplitude of the positive spike waveform. The onset of movement activity was defined as the first of three consecutive bins that exceeded 1 s.d. of the baseline activity. Peak activity was the average firing rate during five 20-ms bins centered at the peak; the peak activity of the nonpreferred movement was acquired from the time window corresponding to the peak bins of preferred movement.

The direction specificity was defined as $\frac{P-NP}{P+NP}$, where P is the firing activity in the preferred direction (pull/push) and NP is firing activity in the nonpreferred direction. Likewise, the size specificity was defined as $\frac{L-S}{L+S}$, where S is the firing activity for small pull movement (<90% of full lever shift) and L is the firing activity for large pull movement (>90%). The velocity specificity was defined as $\frac{F-S}{F+S}$, where S is the firing activity for the slower half of pull movements and F is the firing activity for the faster half of pull movements. The significance of the direction, size or velocity specificity was judged in individual neurons using a Mann-Whitney U test. The relative direction specificity was the direction specificity of one neuron, where a standard (positive) direction was the preferred direction of another neuron. The putative monosynaptic excitatory connectivity in a neuron pair was judged by a single asymmetric peak, its short latency (<2.5 ms) with small jitter (<2 ms) and larger amplitude (>3 s.d.; mean, 13.9 s.d.) than the baseline level (±5 to 25 ms) in cross-correlation histogram (as verified in **Supplementary Fig. 8**)[27–31].

50. Hazan, L., Zugaro, M. & Buzsáki, G. Klusters, NeuroScope, NDManager: A free software suite for neurophysiological data processing and visualization. *J. Neurosci. Methods* **155**, 207–216 (2006).

doi:10.1038/nn.2431